Translocation dynamics of sorting nexin 27 in activated T cells

Esther Rincón[1], Julia Sáez de Guinoa[2], Severine I. Gharbi[1], Carlos O. S. Sorzano[3], Yolanda R. Carrasco[2] and Isabel Mérida[1],*

[1]Lipid signalling Laboratory, Centro Nacional de Biotecnología (CNB)/CSIC, E-28049 Madrid, Spain
[2]B cell Dynamics Laboratory, Department of Immunology and Oncology, Centro Nacional de Biotecnología (CNB)/CSIC, E-28049 Madrid, Spain
[3]Biocomputing Unit, Centro Nacional de Biotecnología (CNB)/CSIC, E-28049 Madrid, Spain
*Author for correspondence (imerida@cnb.csic.es)

Summary

Sorting nexin 27 (SNX27) belongs to the sorting nexin family of proteins, which participate in vesicular and protein trafficking. Similarly to all sorting nexin proteins, SNX27 has a functional PX domain that is important for endosome binding, but it is the only sorting nexin with a PDZ domain. We identified SNX27 as a partner of diacylglycerol kinase ζ (DGKζ), a negative regulator of T cell function that metabolises diacylglycerol to yield phosphatidic acid. SNX27 interacts with the DGKζ PDZ-binding motif in early/recycling endosomes in resting T cells; however, the dynamics and mechanisms underlying SNX27 subcellular localisation during T cell activation are unknown. We demonstrate that in T cells that encounter pulsed antigen-presenting cells, SNX27 in transit on early/recycling endosomes polarise to the immunological synapse. A fraction of SNX27 accumulates at the mature immunological synapse in a process that is dependent on vesicular trafficking, binding of the PX domain to phosphatidylinositol 3-phosphate and the presence of the PDZ region. Downmodulation of expression of either SNX27 or DGKζ results in enhanced basal and antigen-triggered ERK phosphorylation. These results identify SNX27 as a PDZ-containing component of the T cell immunological synapse, and demonstrate a role for this protein in the regulation of the Ras–ERK pathway, suggesting a functional relationship between SNX27 and DGKζ.

Key words: Sorting nexins, PDZ, Membrane trafficking, T cells, Immunological synapse, Diacylglycerol kinase

Introduction

Generation of the immune response requires the formation of a specialised contact area between T cells and antigen-presenting cells (APCs) at the immunological synapse (Friedl et al., 2005). After establishing contact with APCs, T cells acquire a polarised phenotype, characterised by the orientation of the endocytic and secretory machineries, together with the microtubule-organising centre (MTOC), toward the cell–cell contact zone (Billadeau et al., 2007; Cemerski and Shaw, 2006). One function of this repositioning to the immunological synapse is to direct T-cell-secreted cytokines, including interleukin-2 and interferon-γ, to the bound APC (Huse et al., 2006; Huse et al., 2008); in cytotoxic T cells, secretory granules are also delivered by this means (Blott and Griffiths, 2002). Another effect is to guarantee correct formation of the immunological synapse through endocytosis and exocytosis from the recycling pathway (Cemerski and Shaw, 2006), which regulates appropriate expression of specific proteins that accumulate in this zone, such as the T cell antigen receptor (TCR), co-receptors and signalling molecules (Das et al., 2004; Ehrlich et al., 2002; Lee et al., 2003).

The sorting nexins are a large protein family that participate in vesicular and protein trafficking. Over 33 mammalian sorting nexins have been identified and are thought to regulate distinct steps in vesicular trafficking, generally through spatial association with lipid or protein partners (Carlton et al., 2005; Cullen, 2008; Worby and Dixon, 2002). We recently identified SNX27 in early and recycling endosomes in T cells (Rincon et al., 2007). This protein has a specific phox homology (PX) region that is the signature of all sorting nexin family members (Worby and Dixon,

2002). SNX27 is the only member of this group that has a PDZ [post-synaptic density protein (PSD), disc-large and zonula occludens-1] domain, as well as a Ras association (RA) and a FERM (4.1 protein, ezrin, radixin, moesin) domain, which overlap considerably (Cullen, 2008). SNX27 is thought to target its partners to the early endosomal fraction through PDZ-mediated interaction, as reported for SNX27 binding partners such as the 5-hydroxytriptamine type-4 (a) (5-HT$_{4(a)}$) receptor (Joubert et al., 2004), the cytohesin-associated scaffolding protein (CASP) (MacNeil et al., 2007) and G-protein-gated potassium (Kir.3) channels (Lunn et al., 2007).

Our previous experiments identified SNX27 as a protein that interacts with diacylglycerol kinase ζ (DGKζ); this interaction is dependent on the SNX27 PDZ domain (Rincon et al., 2007). DGKζ is a member of the extensive DGK family of enzymes that metabolise diacylglycerol (DAG) into phosphatidic acid. In T cells, DGKζ functions as a negative regulator of Ras activation by limiting the DAG-dependent activation of Ras guanyl nucleotide-releasing protein 1 (RasGRP1), a Ras exchange factor that is selectively expressed in T cells (Olenchock et al., 2006; Zhong et al., 2003; Zhong et al., 2002). DGKζ is transported rapidly to the plasma membrane following stimulation of an ectopically expressed, G-protein-coupled, muscarinic type I receptor (M1R) that is known to mimic TCR responses in T cells (Santos et al., 2002). This translocation is dependent on phosphorylation of the protein-kinase-C-driven MARCKS (myristoylated alanine-rich C kinase substrate) domain and intact zinc fingers. In addition, the presence of a PDZ-binding motif at the DGKζ C-terminus suggests that PDZ interactions participate in targeting of DGKζ to membrane compartments.

Accordingly, DGKζ interacts with several PDZ-containing proteins, including syntrophin (Hogan et al., 2001), TIP15 (Fabre et al., 2000) and PSD-95 (Kim et al., 2009). We showed colocalisation of DGKζ and SXN27 at microsomal compartments, which suggests a role for PDZ interaction at this site (Rincon et al., 2007). The characterisation of a SNX27–DGKζ complex provided a putative role for DGKζ as a negative regulator of recycling endosomal compartments, as DGKζ knockdown cells showed enhanced transferrin receptor recycling (Rincon et al., 2007).

We previously characterised SNX27 in resting T cells (Rincon et al., 2007), but the dynamics and mechanisms underlying SNX27 subcellular localisation during T cell activation have not been described. We analysed SNX27 regulation following T cell activation, and show using superantigen (SEE)-pulsed APCs that SNX27 polarised in endocytic/recycling endosomes to the contact zone of T cells that encountered an APC. A fraction of this protein accumulated at the mature immunological synapse through a mechanism that is dependent on the synergistic function of the PX and PDZ domains. Because SNX27 and DGKζ interact in a PDZ-dependent manner, we studied regulation of these proteins after antigen presentation. Our results reveal that when overexpressed, DGKζ appeared to recruit SNX27 to the plasma membrane, consequently reducing the specific pool of SNX27 at the immunological synapse. However, downmodulation of either SNX27 or DGKζ resulted in enhanced phosphorylation of ERK (extracellular signal regulated kinase), suggesting a functional relationship between these two proteins. In summary, our results identify SNX27 as a component of the T cell immunological synapse, which could regulate protein trafficking through PDZ-mediated interactions, and reveal a role for this protein in the control of Ras activation.

Results
### SNX27 polarises to the T cell synapse in response to TCR triggering
To determine whether SNX27 was regulated by triggering of TCRs, we examined the localisation of GFP–SNX27 in an in vitro model of TCR activation using transiently transfected Jurkat T cells plated on anti-CD3 or anti-CD28 antibodies (van der Merwe, 2002), and GFP–RasGRP1 as a control. We observed that, whereas GFP–RasGRP1 translocates to the plasma membrane in these conditions (Sanjuan et al., 2003), GFP–SNX27 was unable to do so, and instead remained in vesicular structures (Fig. 1A, left). Integrins are an important family of molecules with costimulatory properties (Wang et al., 2010); however, we observed no relocalisation of GFP–SNX27 when cells were plated on integrin fibronectin (Fig. 1A, right).

As an alternative form of stimulation, we incubated Jurkat cells with antibody-coated beads. We labelled Jurkat cells with transferrin tetramethylrhodamine (Tf-Rhod) to track the early/recycling endosomal compartment (Maxfield and McGraw, 2004), and compared GFP–SNX27 translocation with that of GFP–RasGRP1. As predicted, RasGRP1 accumulated at the bead-contact area (Carrasco and Merida, 2004), and the Tf-Rhod-positive compartment polarised to the activation site (Das et al., 2004) (Fig. 1B, top). Under these conditions, GFP–SNX27-positive vesicles colocalised with Tf-Rhod and polarised to the T cell synapse as part of this endosomal compartment (Fig. 1B, bottom), but did not colocalise with markers of the immunological synapse, such as RasGRP1.

SNX27 is recruited to the immunological synapse
We next tested a more physiological system of T cell activation with a model of antigen presentation (Friedl and Storim, 2004), using Raji B cells alone or pulsed with the *Staphylococcal* enterotoxin E (SEE) superantigen (Fraser et al., 2000). The formation of cell–cell conjugates was analysed both by immunofluorescence and videomicroscopy. As a control for synapse accumulation, we examined cells transfected with GFP–PKCθ, which relocates to the T cell synapse (Monks et al., 1997) (Fig. 2A, left column). When Jurkat T cells were incubated with SEE-pulsed APCs, SNX27-rich compartments polarised rapidly to the cell contact zone, with a SNX27 fraction
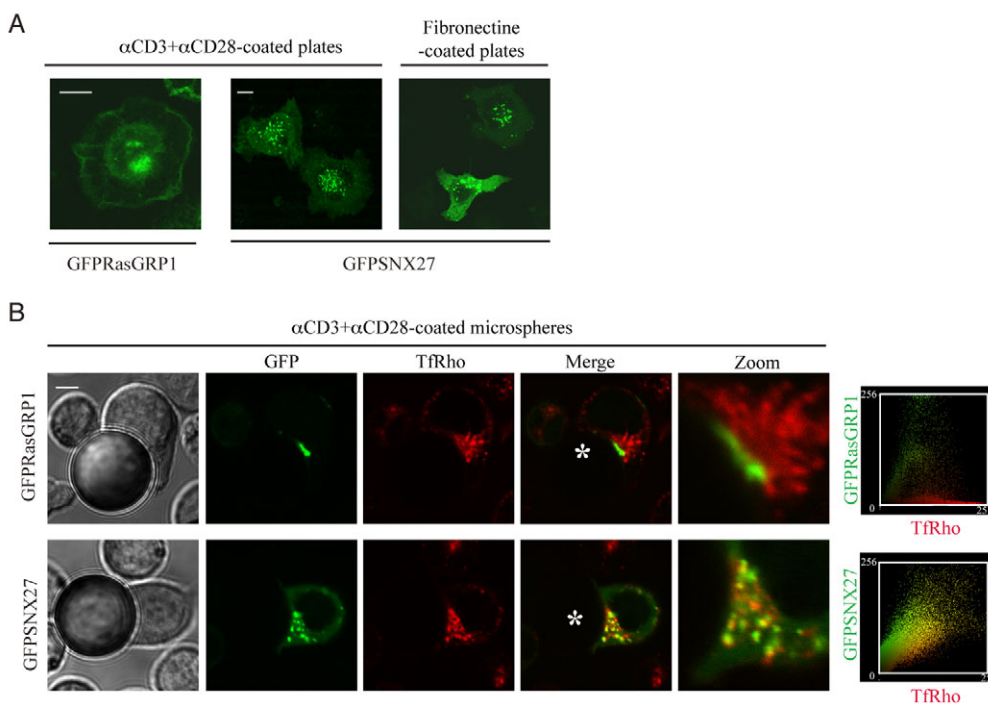
Fig. 1. Stimulation with antibodies against CD3 and CD28 induces SNX27 polarisation under conditions of synapse formation. Transiently transfected Jurkat T were transferred to anti-CD3 and anti-CD28 antibody or fibronectin-coated chambered coverslips (**A**), or treated with Tf-Rhod, suspended in HBSS, and mixed with microspheres coated with anti-CD3 and anti-CD28 antibodies a 1:1 cell:bead ratio and plated on poly-L-lysine-coated chambers (**B**). Slides were mounted on a 37°C plate and images were directly acquired by confocal microscopy. The asterisk marks the bead position. The plots on the right show Pearson's correlation coefficient between SNX27 and Tf-Rhod (=0.831) and RasGRP and Tf-Rhod (=0.185). Scale bars: 3 μm.

accumulating at the immunological synapse, similarly to PKCθ (Fig. 2A, right column). To analyse in more detail the apparent existence of two SNX27 pools at two distinct sites, we determined the percentage of cells showing GFP–SNX27 accumulation at the T-cell–APC contact zone. GFP–SNX27 localised at the immunological synapse in 86% of cells (Fig. 2A; Fig. 2B, top panel) amongst which only 60% also showed polarisation of vesicular compartments (Fig. 2Ae; Fig. 2B, top panel). Quantification of the amount of GFP–SNX27 clustered at the synapse (determined as fluorescence intensity at the immunological synapse/total fluorescence) showed that GFP–SNX27 accumulation at the synapse was higher in cells with polarised vesicular compartment (Fig. 2B, bottom panel). Endogenous SNX27 showed a similar vesicle localisation in the presence of unpulsed or pulsed APCs (Fig. 2C). This could suggest that relocalisation of SNX27-rich vesicular compartments occurs in a dynamic way and that they migrate towards the site of cell–cell contact at the the immunological synapse.

To corroborate this hypothesis, we next used videomicroscopy to examine the dynamic relocalisation of GFP–SNX27 during synapse formation. We observed rapid, clear polarisation of SNX27-positive vesicles to the T-cell–APC contact area, followed shortly thereafter by accumulation of GFP–SNX27 at the contact zone (Fig. 2D and supplementary material Movie 1). This happened from the second minute of SEE-pulsed APC contact, which coincides with the formation of a mature immunological synapse (Friedl and Gunzer, 2001).

These experiments suggest that SNX27 is associated with vesicle compartments; after antigen presentation, the endocytic compartment is polarised and an SNX27-rich pool is further recruited to the plasma membrane at the contact zone.

Recruitment of SNX27 to the immunological synapse is dependent on early or recycling endosome machinery

Protein in vesicle structures can reach the plasma membrane in a highly regulated manner through specific cellular
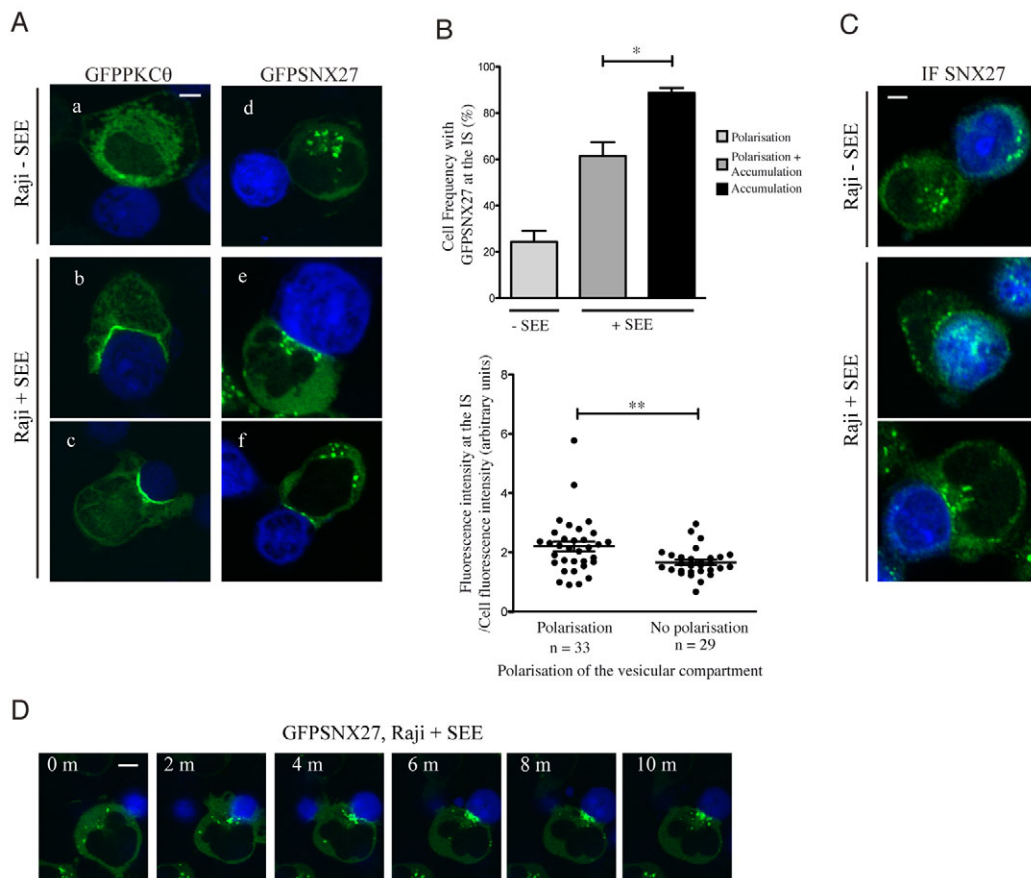
Fig. 2. SNX27 is recruited to the immunological synapse in Jurkat T cells stimulated with SEE-pulsed APCs. (A) GFP–PKCθ- or GFP–SNX27-transfected Jurkat T cells were stimulated with APCs at a 1:1 Jurkat:APC ratio. Cell–cell conjugates were fixed and images acquired by confocal microscopy. (B) Top graph shows quantification of cells with GFP–SNX27 polarisation and/or accumulation at the immunological synapse. In the presence of SEE-pulsed APCs, 86% of the cell population show GFP–SNX27 accumulation at the immunological synapse. Of this percentage, 60% of cells also showed polarisation of vesicular compartments (see a representative image in Ae), whereas in the rest there was accumulation at the immunological synapse in the absence of vesicular compartment polarisation (see representative image in Af). Data are presented as the means ± s.e.m. of cell frequency with GFP–SNX27 relocated to the immunological synapse in three independent experiments (n>100 in each experiment) (*P<0.05; Student's t-test). Bottom graph shows quantitative image analysis of GFP–SNX27 accumulated at the immunological synapse compared with total GFP–SNX27. Each dot represents a T-cell–APC conjugate. The bars show the means ± s.e.m. (**P<0.01; Kolmogorov-Smirnov test). (C) Jurkat T cells were stimulated with APCs as in A, and endogenous SNX27 was detected with anti-SNX27 and secondary antibody coupled to Alexa Fluor 488. (D) Transiently transfected Jurkat T cells were allowed to attach to poly-L-lysine-coated chamber slides. Slides were mounted on heated microscope stage and images were acquired by time-lapse microscopy and SEE-pulsed APCs were added to monitor the formation of conjugates. The figure shows representative images from time 0 to 10 minutes after stimulation. Supplementary material Movie 1 shows all stimulation period images. Scale bars: 3 μm.

subcompartments (Blott and Griffiths, 2002; Maxfield and McGraw, 2004). To determine the mechanism of translocation of SNX27 to the immunological synapse, we next stained GFP–SNX27-transfected cells with several markers of vesicular trafficking. We used Tf-Rhod as a marker of the endocytic recycling compartment (Maxfield and McGraw, 2004), SNX2 as an early endosomal marker (Gullapalli et al., 2004) and Lamp1 as a marker of the lysosomal and secretory compartments (Blott and Griffiths, 2002; Chen et al., 1988). A fraction of GFP–SNX27 colocalised with Tf-Rhod- and SNX2-positive vesicles that polarise to the T cell synapse in the presence of SEE-pulsed APCs (Fig. 3A, top and middle rows), further corroborating the presence of SNX27 in recycling/early endosomal compartments, whereas there was no colocalisation between SNX27 and lysosomal/secretory compartments (Fig. 3A, bottom). However, although all the vesicular compartment markers tested polarised towards the cell contact zone, none of them showed direct accumulation at the immunological synapse with GFP–SNX27 (Fig. 3A, arrows).

To further assess whether immunological synapse localisation of GFP–SNX27 required vesicular trafficking, Jurkat cells were pretreated with primaquine, which inhibits secretion and recycling processes through irreversible inactivation of the transport vesicles (donors), but not of final membranes (acceptors) (Hiebsch et al., 1991; Somasundaram et al., 1995; van Weert et al., 2000). When primaquine-treated Jurkat T cells were incubated with SEE-pulsed APCs, we observed a marked reduction of the fluorescence intensity of GFP–SNX27 at the immunological synapse that accumulated in recycling endosomes, and colocalised with the transferrin receptor (TfR) (Fig. 3B). These results, which are similar to those describing primaquine-dependent inhibition of the recycling of TfR (van Weert et al., 2000) and TCR (Das et al., 2004), suggest that trafficking through the endosomal compartment is necessary for SNX27 to reach the T-cell–APC contact zone.

GFP–SNX27 accumulates at central and peripheral SMACs

The experimental systems used, either antibody-coated microspheres or SEE-pulsed B cells, are valid models in which to analyse long-term, stable T cell synapses (Friedl et al., 2005). The mature immunological synapse that originates when T cells contact B cells has been studied extensively, allowing identification and characterisation of various supramolecular activation clusters (SMACs) in the T cell contact area (Fooksman et al., 2010). Early fixed-cell imaging studies revealed the formation of a bull's eye
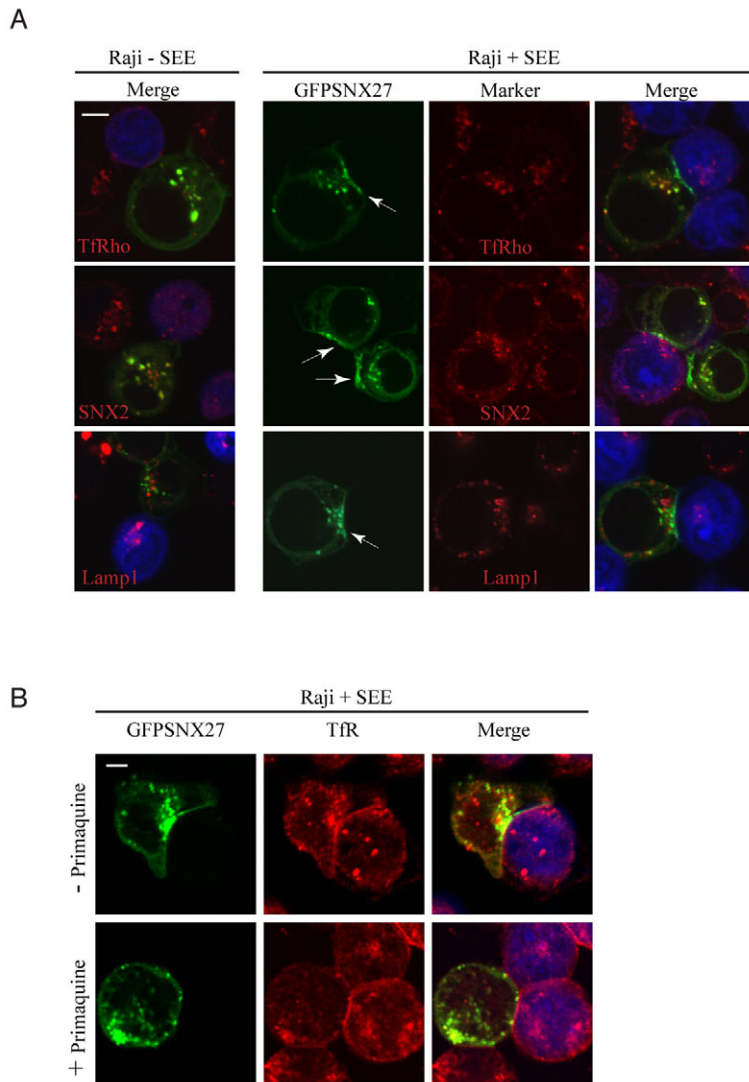
Fig. 3. SNX27 recruitment to the immunological synapse is dependent on early/recycling endosome binding. (A) Transiently transfected Jurkat T cells were treated with Tf-Rhod (top), and stimulated with APCs pulsed or not with SEE, as in Fig. 2A. Immunostaining was carried out with anti-SNX2 (middle) or anti-Lamp1 (bottom), followed by Cy3 anti-mouse IgG antibodies and imaged by confocal microscopy. GFP–SNX27 accumulates at the immunological synapse (see arrows). (B) GFP–SNX27-transfected cells were incubated with medium alone or with primaquine, then mixed with SEE-pulsed Raji B cells, and protein distribution was analysed by immunostaining with anti-TfR followed by Cy3-anti-mouse IgG antibodies and imaged by confocal microscopy. Scale bars: 3 µm.

pattern with a central cluster of TCR-pMHC (peptide-loaded major histocompatibility complex) defined as the central SMAC (cSMAC), surrounded by a ring that contributes to firm adhesion through accumulation of molecules including LFA-1 (lymphocyte function-associated antigen 1) and talin, named the peripheral SMAC (pSMAC). The region outside the pSMAC, which is rich in CD45, was later named the distal SMAC (dSMAC) (Davis et al., 2003; Fooksman et al., 2010; Monks et al., 1998). To determine whether SNX27 is recruited to a specific SMAC at the immunological synapse, we analysed colocalisation of GFP–SNX27 with CD3 or LFA-1, which are well-characterised markers of cSMAC and pSMAC, respectively. We also detected phosphorylated tyrosine, which is increased at the cell–cell contact zone as a result of tyrosine phosphorylation of scaffolding and signalling molecules. GFP–SNX27 translocated to the contact zone and showed clear colocalisation with LFA-1 (Fig. 4A, top). However, en face (y-z) reconstruction of the SMAC structures showed a quite homogeneous distribution of GFP–SNX27 areas, which corresponded to both the cSMAC and pSMAC (Fig. 4A, bottom and supplementary material Movie 2).

Planar lipid bilayers supported on glass coverslips have been used to image the immunological synapse at high resolution (Dustin et al., 2007). Dynamic studies using this system have shown that activating TCR clusters form first in the dSMAC and then move

to the cSMAC region within a few minutes. The sustained TCR signalling that originates at the immunological synapse appears to be the result of a continuous process of cluster formation and transport from the dSMAC to the cSMAC (Fooksman et al., 2010). More recently, a region in the transition between central and peripheral SMAC has been described, which serves as a platform for costimulatory signalling proteins, such as CD28 (Yokosuka et al., 2008). To assess whether the distribution of GFP–SNX27 observed in fixed cells was the result of a dynamic transport between the different SMACs, we determined the localisation of GFP–SNX27 vesicles in the mature immunological synapse generated when Jurkat cells interacted with supported planar lipid bilayers containing GPI-linked ICAM-1 (intercellular adhesion molecule 1) and tethered anti-CD3 antibodies as surrogate antigen (see the Materials and Methods). We used the accumulated anti-CD3 fluorescent signal as a marker for the cSMAC at the mature immunological synapse; the pSMAC area was estimated as the cell–lipid-bilayer contact region (followed by interference reflection microscopy, IRM) surrounding the cSMAC (CD3-positive region). This analysis showed that GFP–SNX27 vesicles reached both the cSMAC and the pSMAC (Fig. 4B and supplementary material Movie 3). It is noteworthy that the merge between GFP–SNX27, CD3 and IRM images, showed that the localisation of GFPSN27 at the pSMAC appears very close to the boundary with the CD3-
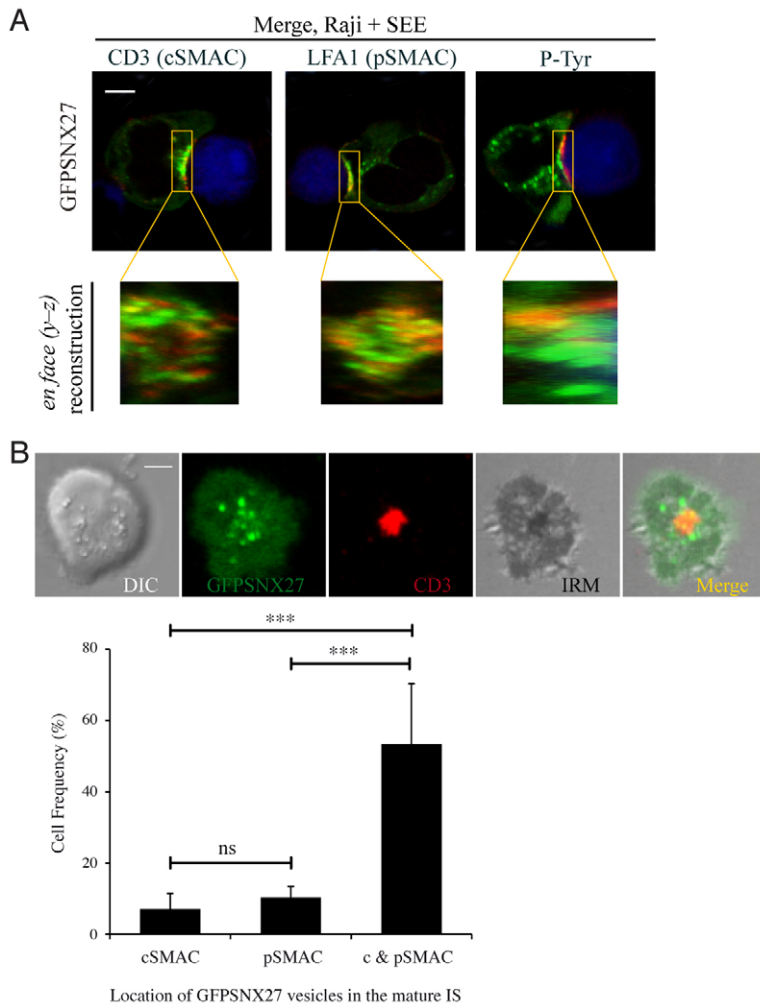
Fig. 4. Distribution of GFP–SNX27 at the Jurkat T cell mature immunological synapse. (A) GFP–SNX27-transfected Jurkat T cells were stimulated with APCs as in Fig. 2A. Cell–cell conjugates were fixed, processed for immunofluorescence with anti-CD3 (first column), anti-LFA1 (second column) or anti-phosphorylated-Tyrosine (third column), followed by Cy3-anti-mouse IgG antibodies and imaged by confocal microscopy. Three-dimensional reconstructions of the SMAC structures are shown in the magnified panels and in supplementary material Movie 2. (B) DIC, fluorescent anti-CD3 and IRM images of a representative GFP–SNX27 transfected Jurkat T cell forming the immunological synapse after anti-CD3 recognition on an ICAM-1 containing lipid bilayer. Graph shows the frequency of Jurkat T cells that exhibited immunological synapse accumulation of GFP–SNX27 vesicles at the indicated locations. Data are presented as the means ± s.e.m. of four experiments (ns, not significant; ***P<0.001; Student's t-test). Scale bars: 3 μm.

positive region or cSMAC (Fig. 4B, top), suggesting the localisation of a SNX27 pool in the costimulatory platform of the mature immunological synapse (Yokosuka et al., 2008).

GFP–SNX27 recruitment to the T cell synapse requires both PX and PDZ domains

To gain further insight into the nature of the signals regulating SNX27, we next examined the input of the different structural domains of SNX27 on its localisation at the immunological synapse. Visual analysis suggested that deletion of the RA-FERM domains had no apparent effect on vesicular localisation of SNX27 or its recruitment to the immunological synapse (Fig. 5A, right, second row). To analyse the contribution of the PX domain, we generated point mutations in the R196,Y197 sequence. This sequence has been shown to interact with phosphatidylinositol 3-phosphate (PI3P), the most abundant phosphatidylinositol derivative in endosomal membranes (Gillooly et al., 2000), with other PX domain-containing proteins such as p40^{phox} (R58,Y59) (Bravo et al., 2001), PLD1 (K119, which is similar to R196) (Stahelin et al., 2004) and SNX3 (R70,Y71) (Xu, 2001) (Fig. 5A, bottom left shows an alignment of PX sequences). As predicted, the PX domain mutant lost vesicular localisation almost completely, although interestingly, a small pool was still able to localise at the cell contact zone (Fig. 5A, right, third row). Finally, we examined a SNX27 construct bearing a deletion of the PDZ domain. As previously reported, this deletion strongly impaired SNX27 targeting to the endocytic compartment (Rincon et al., 2007). When T cells were challenged with SEE-pulsed APCs, the vesicles positive for SNX27 lacking the PDZ motif (GFP–SNX27ΔPDZ) polarised to the cell contact area; however, they did not accumulate at the immunological synapse (Fig. 5A, right, fourth row). Quantitative analysis of accumulation of the distinct mutants (Fig. 5B, black dots) and exclusion (grey dots) at the immunological synapse confirmed that, albeit much lower than in the full-length protein, GFP–SNX27 mutants defective in PI3P binding retained certain ability to localise to the immunological synapse; deletion of the RA domain did not result in significant differences with respect to the wild-type GFP–SNX27 and GFP–SNX27ΔPDZ was always excluded from the immunological synapse.

We next assessed the capacity of mutants bearing a truncation of the PDZ region or with impaired PIP3 binding to reach the immunological synapse in T cells contacting antigen-loaded lipid bilayers. As for fixed cells, the number of GFP–SNX27 vesicles reaching the synapse was strongly reduced if the PDZ domain was truncated (Fig. 5C and supplementary material Fig. S1). As expected, the GFP–SNX27 mutant defective in PIP3 binding did not show vesicle localisation but there was significant frequency of fluorescence accumulation when it was in contact with lipid bilayers (Fig. 5C and supplementary material Fig. S1).

These experiments suggest that deletion of the PDZ region has an important effect on GFP–SNX27 recruitment to the immunological synapse. To test whether PDZ truncation affected PX domain accessibility and PI3P binding, we used a lipid-binding assay. Recombinant proteins expressing GST-fused wild-type SNX27 (GST–SNX27), the PX domain point mutant [GST–SNX27(R196A,Y197A)], or the PDZ region deleted mutant (GST–SNX27ΔPDZ) were generated, purified and overlaid on lipid strips. Analysis with anti-GST antibodies showed proteins of the predicted molecular weight (not shown). GST–SNX27 showed specific PI3P binding (Fig. 5D). Point mutation of the PX domain resulted in complete loss of PI3P binding, whereas PDZ domain truncation did not affect binding to PI3P (Fig. 5D).

Taken together, these results show that the PDZ region does not participate in PI3P binding, and strongly suggest that SNX27 localisation to the immunological synapse requires synergy between the PX domain, which binds to PI3P, and the PDZ domain, which would bind to an as yet uncharacterised protein(s).

### The DGKζ C-terminal region blocks recruitment of SNX27 to the immunological synapse

The previous experiments revealed that PDZ-based interaction was essential for SNX27 recruitment to the immunological synapse. Since our proteomic screen revealed that SNX27 is a direct binding partner of DGKζ (Rincon et al., 2007), we next wanted to study the contribution of DGKζ to the recruitment of SNX27 to the immunological synapse. We examined localisation of SNX27 in cells overexpressing the C-terminal region of DGKζ (HA–DGKζCT), which encompasses the ETAV sequence required for the DGKζ–SNX27 interaction and acts as a dominant negative (Rincon et al., 2007). As reported, cells expressing the HA–DGKζCT construct showed fewer GFP–SNX27-positive vesicles, confirming the relevance of the PDZ domain in this localisation (Rincon et al., 2007 and Fig. 6). Moreover, when cells positive for the HA–DGKζCT were in contact with SEE-pulsed APCs, no recruitment of GFP–SNX27 to the immunological synapse was observed. These experiments suggest that SNX27 requires PDZ-mediated interactions with endogenous proteins to localise to endomembrane compartments, which is necessary to drive SNX27 to the immunological synapse.

To determine the role of endogenous DGKζ on SNX27 polarisation and recruitment, we monitored the translocation of GFP–SNX27 in a gene-silencing experiment by short interfering RNA (siRNA). Jurkat T cells transfected with control siRNA and siRNA to knock down DGKζ were compared by immunofluorescence. Although we achieved good silencing efficiency of DGKζ, no significant difference in GFP–SNX27 recruitment was observed (supplementary material Fig. S2).

Role of DGKζ in the regulation of SNX27 translocation in response to antigen presentation

The previous results suggest that DGKζ is not the protein responsible for SNX27 accumulation at the immunological synapse. Moreover, overexpression of the DGKζ sequence responsible for this interaction impairs accumulation of GFP–SNX27 at the contact zone. We coexpressed GFP–SNX27 with DGKζ tagged with the red fluorescent protein (RFP) to check their colocalisation. In basal conditions, DGKζ and SNX27 shared strong overlap in subcellular localisation, which was lost when we coexpressed the mutant of DGKζ deficient in the PDZ binding domain, thus suggesting that this colocalisation requires PDZ-mediated interaction (Fig. 7A). This observation correlated with our previous report showing that both proteins colocalise in internal membranes (Rincon et al., 2007).

To further study whether SNX27 and DGKζ interaction was maintained during T-cell–APC contact, we then followed their redistribution during immunological synapse formation. As expected, GFP–SNX27 translocated to the immunological synapse when cotransfected with empty RFP vector (Fig. 7B, top). GFP–SNX27 recruitment to the immunological synapse was less pronounced when cotransfected with RFP–DGKζ, but instead, we observed a clear relocalisation of SNX27 to the whole plasma
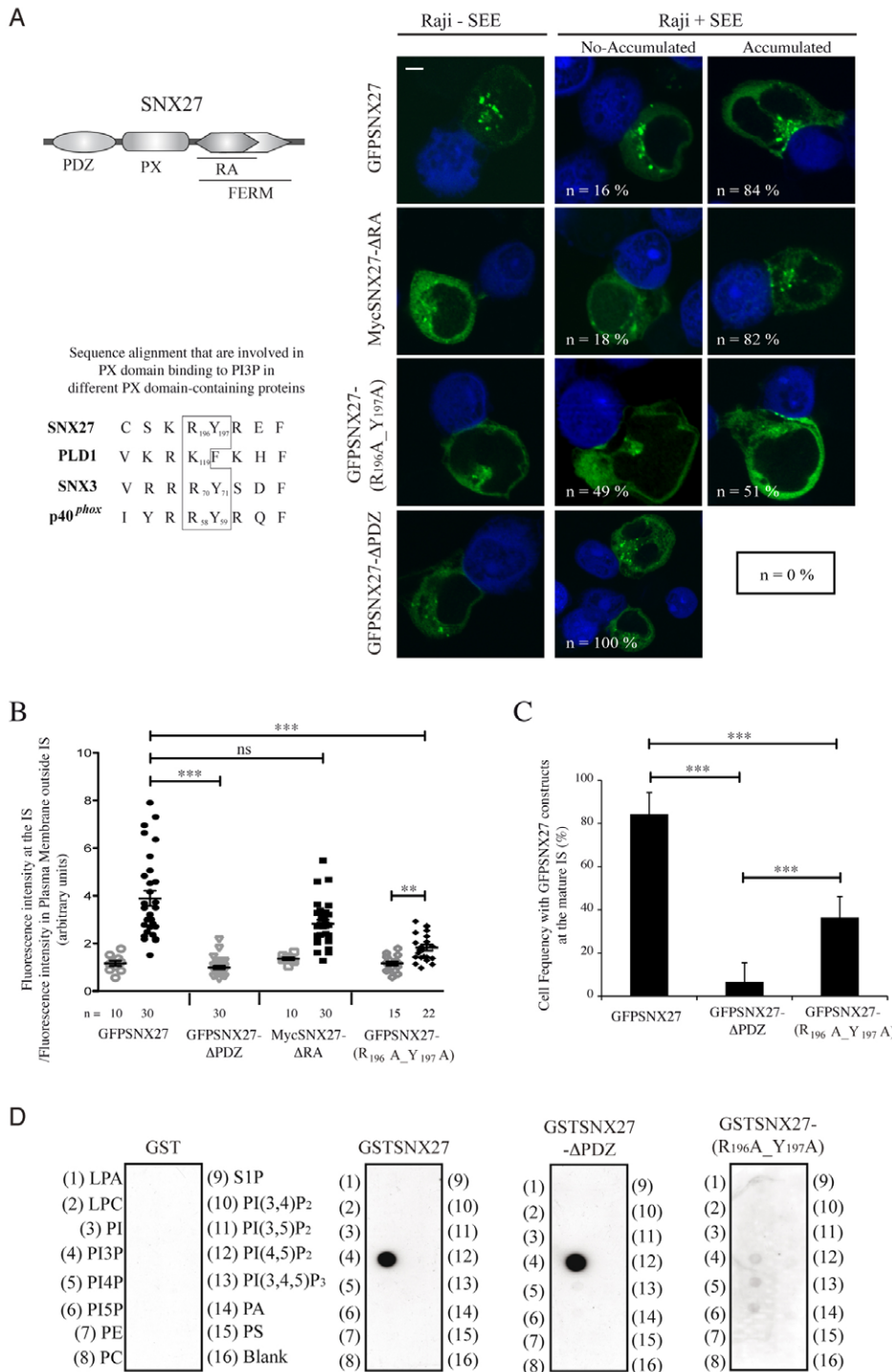
Fig. 5. GFP–SNX27 recruitment to the immunological synapse requires PI3P binding through the PX domain and presence of the PDZ domain. (**A**) Top left drawing shows the SNX27 domains. Micrographs on the right show Jurkat T cells transfected with GFP–SNX27, MycSNX27ΔRA, a construct with RA and FERM domains deleted, GFP–SNX27(R196A,Y197A), a construct with point mutations to alanine in the residues R196,Y197 and GFP–SNX27ΔPDZ, a mutant in which the PDZ domain is deleted. Cells were stimulated with APCs pulsed or not with SEE, as in Fig. 2A, fixed and imaged by confocal microscopy. MycSNX27ΔRA, was detected with anti-Myc, followed by Cy3-anti-mouse IgG antibody. The frequency of T cells with GFP–SNX27 accumulation at the immunological synapse is shown in each image ($n > 100$ cells). Scale bar: 3 μm. Sequence alignment with other PX-domain-containing proteins is shown on the left. (**B**) Quantitative image analysis of GFP–SNX27 accumulated at the immunological synapse compared with GFP–SNX27 located in plasma membrane regions outside the immunological synapse. Each dot represents a T-cell–APC conjugate: empty grey dots represent cells with no accumulation of GFP–SNX27 constructs at the immunological synapse (representative images are shown in A, middle column); solid black dots represent cells with GFP–SNX27 construct accumulation (representative images shown in A, right column). The bars show the means ± s.e.m. (ns, not significant; **$P < 0.01$; ***$P < 0.001$; Kolmogorov–Smirnov test). (**C**) Frequency of transfected Jurkat T cells that accumulate GFP–SNX27 constructs at the immunological synapse after anti-CD3 recognition on an ICAM-1-containing lipid bilayer. The data show the mean of two experiments ± s.e.m. (***$P < 0.001$; Student's t-test). (**D**) Full-length SNX27, SNX27ΔPDZ and SNX27(R196A,Y197A) fused to GST tag were incubated with PIP strips and detected with anti-GST antibody. LPA, lysophosphatidic acid; LPC, lysophosphatidylcholine; PI, phosphatidylinositol; PI3P, PI4P, PI5P, phosphatidylinositol phosphorylated in positions 3, 4, 5; PE, phosphatidylethanolamine; PC, phosphatidylcholine; S1P, sphingosine-1-phosphate; PA, phosphatidic acid; PS, phosphatidylserine.

membrane, mimicking the behaviour of RFP–DGKζ. Line-scan analysis confirmed that GFP–SNX27 colocalised with RFP–DGKζ to the entire plasma membrane, suggesting that DGKζ overexpression recruited SNX27 to this localisation (Fig. 7B, middle). Interestingly, coexpression with RFP–DGKζΔPDZbm did not affect the subcellular localisation of GFP–SNX27, which remained in vesicles and reached the immunological synapse, similarly to the control condition (Fig. 7B, top), although this PDZ-deficient mutant could translocate to the membrane upon T cell activation (Fig. 7B, bottom). This correlates with our observation that HA-DGKζCT blocked recruitment of SNX27 to the immunological synapse, and suggests that DGKζ can compete for SNX27 interaction with other proteins at the immunological synapse.

SNX27 silencing results in enhanced TCR-mediated Ras–ERK activation

The previous experiments demonstrate that, whereas both proteins colocalise under resting conditions, DGKζ relocates to the plasma membrane following formation of the immunological synapse, and
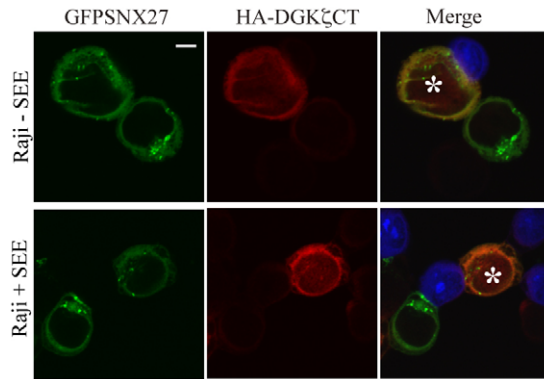
Fig. 6. The DGKζ CT region blocks SNX27 accumulation at the immunological synapse. Jurkat T cells were cotransfected with GFP–SNX27 and a plasmid encoding the DGKζ CT region fused to a HA tag. At 24 hours after transfection, cells were stimulated with APCs as in Fig. 2A, fixed, stained with anti-HA followed by Cy3-anti-mouse IgG antibodies and imaged by confocal microscopy. SNX27 localisation in cells expressing both proteins (asterisk) compared with that in cells not expressing the HA-DGKζ construct showed clear inhibition of GFP–SNX27 accumulation at the immunological synapse in the former. Scale bar: 3 μm.

SNX27 accumulates at the cell–cell contact area. This correlates with the fact that GFP–SNX27 accumulation at the immunological synapse, although it requires intact PX and PDZ regions, is not affected by downmodulation of DGKζ. This somewhat puzzling scenario suggests that, upon T-cell–APC contact, the interaction between the two proteins is disrupted. Localisation studies did not allow us to draw any conclusion regarding a functional relationship between these two proteins.

Studies in Jurkat cells have shown that overexpression of DGKζ limits the threshold of Ras activation by metabolising the DAG that binds to and activates RasGRP1 (Roose et al., 2005). We determined the role of endogenous SNX27 on TCR-mediated activation of Ras by measuring ERK phosphorylation in SNX27-silenced cells using short interfering RNA (siRNA). Jurkat T cells transfected with control siRNA showed marked ERK phosphorylation 15 minutes after TCR triggering (Fig. 8). Silencing of DGKζ resulted in enhanced ERK phosphorylation, confirming the negative function of this lipid kinase in the regulation of this pathway. Longer exposures showed enhanced phosphorylation, even in the absence of TCR triggering, confirming a role for DAG metabolism in the regulation of RasGRP1 (Roose et al., 2007). Downmodulation of SNX27 levels showed a similar increase in ERK phosphorylation both before and after TCR stimulation. (Fig. 8B). These results indicate a functional relationship between the two proteins and suggest that SNX27 is required for adequate downregulation of the Ras–ERK pathway by DGKζ.

Discussion

The sorting nexins are a large family of proteins defined by the presence of a PX domain. Some of these proteins can link endosomal sorting with specific signalling events. SNX27 is suggested to be one such protein, because it contains recognised signalling domains such as the RA and the PDZ (Cullen, 2008). Here we show that SNX27 is transported in early or recycling endosomes that polarise to the T cell synapse, a large signalling molecule platform (Cemerski and Shaw, 2006). In addition, we found that a fraction of SNX27 is recruited to the immunological

synapse by a mechanism that depends on vesicle trafficking, and characterised the SNX27 PDZ region as essential in the control of this accumulation.

Our studies show that SNX27-positive endosomes polarise to the immunological synapse in response to TCR activation, similarly to SNX27 polarisation in migrating and tumour-engaged natural killer cells (MacNeil and Pohajdak, 2007). In addition, an SNX27 pool is recruited to the cell–cell contact area within ~2–3 minutes after an encounter with pulsed APCs. These results are reminiscent of studies showing that components of the TCR signalling machinery (including LAT, p56lck and CD3, which similarly to SNX27 codistribute with transferrin) are recruited to the immunological synapse with kinetics similar to that observed here (Anton et al., 2008; Bonello et al., 2004; Das et al., 2004; Ehrlich et al., 2002). The subcellular distribution of GFP–SNX27 resembled that of endogenous SNX27, which excludes artefacts caused by the GFP tag. The results obtained using the planar lipid bilayer approach, show the localisation of GFP–SNX27 at the cSMAC, but also at the pSMAC, where GFP–SNX27-positive vesicles are distributed very close to the transition region with the cSMAC, an area recently described as the costimulation platform for T cell activation (Yokosuka et al., 2008). These data confirm the concentration of SNX27 at the immunological synapse and suggest its participation as a component of some signalling platforms that remain to be fully characterised.

Analysis of several SNX27 mutants confirmed that the SNX27 PX domain is necessary for vesicle localisation, collaborates in immunological synapse accumulation, and binds PI3P lipids, confirming its role in vesicle binding (Gillooly et al., 2000). The PX domain is the signature of the sorting nexin family, but other family members as we show for SNX2, do not accumulate at this site. This is, to our knowledge, the first report of immunological synapse recruitment for a sorting nexin, although studies in T cells by Badour and co-workers show that SNX9 interacts simultaneously with WASp (Wiskott–Aldrich syndrome protein) through its Src homology 3 domain and with PI3-kinase through its PX domain. The formation of this complex regulates internalisation of CD28 and activation of NFAT (nuclear factor of activated T cells) (Badour et al., 2007). SNX27 is the only family member with a PDZ domain (Cullen, 2008) and our analyses show that this region is essential for both its endosomal distribution and its recruitment to the immunological synapse. This is not due to phosphatidylinositol binding, which we have shown is dependent exclusively on the PX region. Together, our data suggest that SNX27 participates in PDZ-mediated protein sorting to the immunological synapse. We searched extensively for SNX27-interacting proteins at the immunological synapse, but have not detected a suitable candidate. Identification of additional SNX27 partners will help to elucidate additional functions of this protein during T cell stimulation.

The PDZ domain is a well-characterised protein–protein interaction module (Sheng and Sala, 2001); in fact, several SNX27 partners containing PDZ binding motifs have been characterised in lymphoid and non-lymphoid cells. Elegant studies in neurons have shown that SNX27 interacts with Kir3.3 and Kir3.2c potassium channels, which promotes their trafficking to endosomes and leads to smaller Kir3 potassium currents (Lunn et al., 2007). SNX27 also targets the 5-HT$_{4(a)}$ receptor to endosomal compartments (Joubert et al., 2004). Studies in the natural killer T cell line YT showed that SNX27 interacts with CASP, a cytokine-inducible protein that associates with members of the GEF
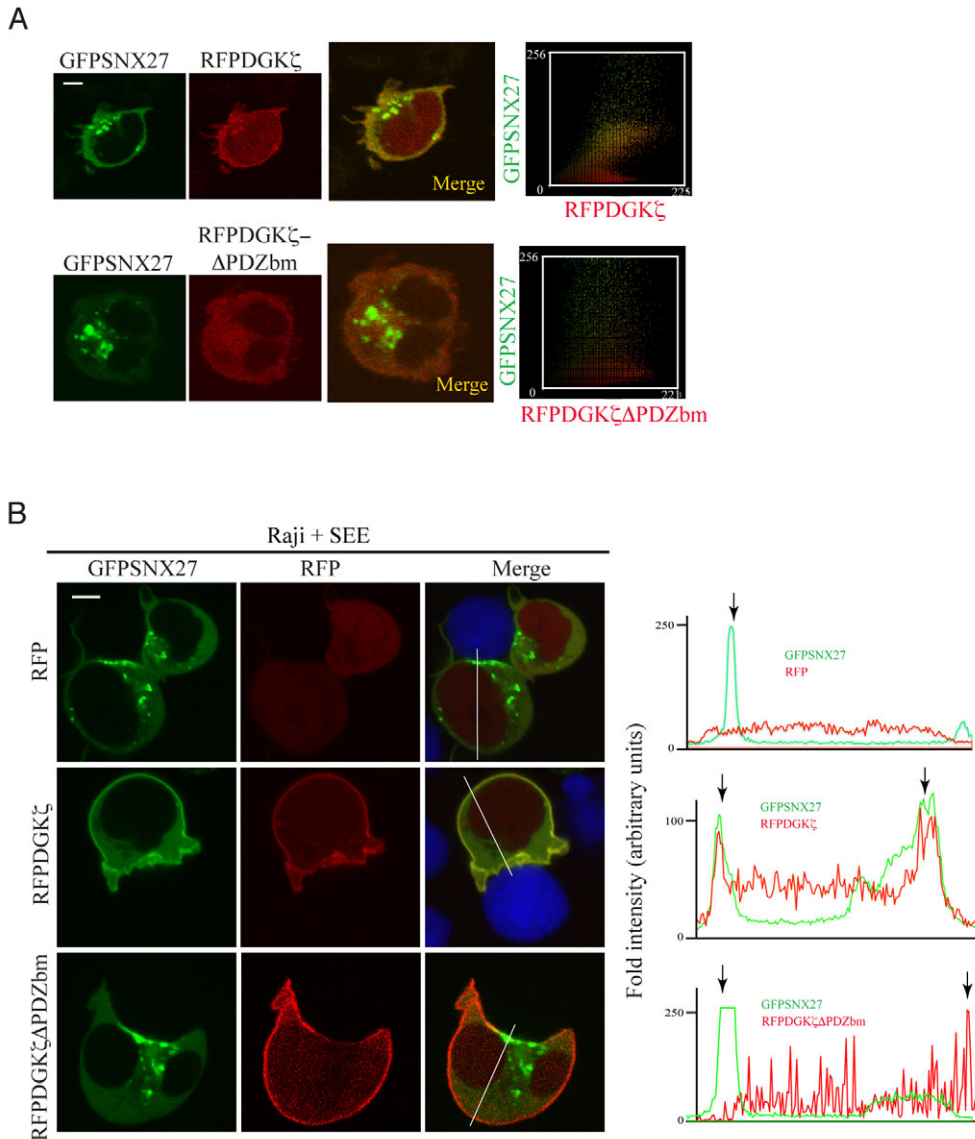
Fig. 7. DGKζ recruits SNX27 in a PDZbm-dependent manner to the entire plasma membrane in Jurkat T cells stimulated with SEE-pulsed APCs. (A) Jurkat T cells were cotransfected with GFP–SNX27 and RFP–DGKζ or RFP–DGKζΔPDZbm, fixed and imaged by confocal microscopy. Pearson's correlation coefficients were 0.778 for GFP–SNX27/RFP–DGKζ and 0.576 for GFP–SNX27/RFP–DGKζΔPDZbm. (B) Densitometric analysis of the distribution of GFP–SNX27 and RFP, RFP–DGKζ or RFP–DGKζΔPDZbm constructs along the line in each type of cells is shown in the panels on the right. Arrows indicate the position of the periphery of the cells. Scale bars: 3 μm.

cytohesin family. These results suggest that endosomal SNX27 recruits CASP, although there are no further data on the functional role of this interaction (MacNeil et al., 2007). It is noteworthy that all SNX27 partners identified are closely related to the neuronal and immunological systems (MacNeil et al., 2007; Rincon et al., 2007). These two tissues showed specific expression of genes that encode PDZ-containing proteins (Giallourakis et al., 2006). The role of PDZ-containing protein in neuronal tissues is well documented. They are enriched in the neuronal synapse where they regulate synapse composition, thereby determining its size and strength (Kim and Sheng, 2004). Although somewhat unexpected, the large number of PDZ-containing proteins in immune tissue suggests an important function at this site (Giallourakis et al., 2006). Recruitment of hDlg (human Discs large) to the immunological synapse, for example, regulates T cell function and polarity by specific recruitment of PDZbm-containing proteins (Ludford-Menting et al., 2005). Our data identify SNX27 as a PDZ component of the T cell immunological synapse. Immunofluorescence analysis with an anti-hDlg antibody showed no colocalisation with SNX27 at the immunological synapse (not

shown), suggesting that SNX27 and hDlg form part of distinct protein complexes.

Our earlier data describing the interaction between SNX27 and DGKζ in T cells (Rincon et al., 2007) prompted us to investigate the functional relationship of these two proteins. Following overexpression of the DGKζ C-terminal region, localisation of SNX27 to the immunological synapse was lost, although it was unaffected by DGKζ downmodulation, confirming the presence of additional SNX27 partners that interact at this site. Microscopy analysis reveals a PDZ-mediated interaction between DGKζ and SNX27. Interestingly, DGKζ shuttles to the plasma membrane in response to T cell engagement and its overexpression was sufficient to dislodge SNX27 from an immunological synapse pool and to send it to the whole plasma membrane. This would suggest that there is a tight regulation between these two proteins and that they can reciprocally alter their localisation and activation. We were not able to detect specific recruitment of DGKζ to the immunological synapse, although it is possible that SNX27 directs localisation of DGKζ to this site. Our silencing estimation showed that, although DGKζ was not necessary to direct SNX27 to the immunological
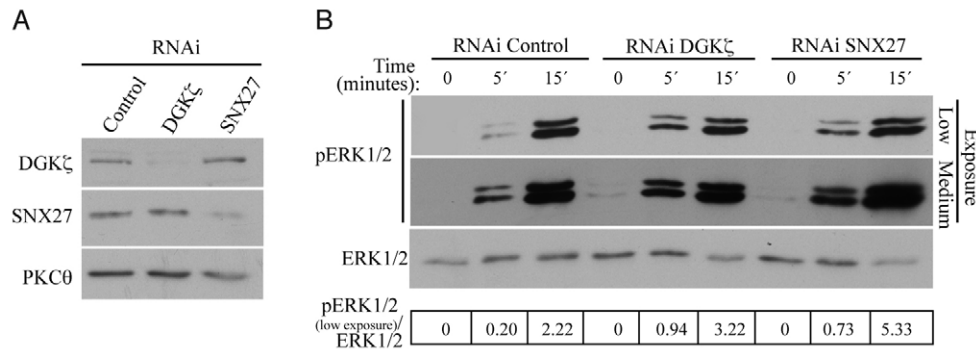
Fig. 8. Enhanced ERK phosphorylation in Jurkat T cells with knockdown of DGKζ or SNX27. Jurkat T cells were transfected with siRNA control, siRNA against SNX27 or DGKζ and collected 3 days after transfection. (**A**) RNAi efficiency was evaluated by western blotting with rabbit anti-DGKζ or anti-SNX27; anti-PKCθ was used as a control. (**B**) Silenced Jurkat cells were stimulated with unpulsed APCs (time 0) or SEE-pulsed APCs (5 and 15 minutes) and phosphorylation of ERK1/2 was evaluated using specific antibody (top and middle panels). Blot was reprobed with anti-ERK1/2 (bottom panel). Normalised values of perk to ERK were quantified using ImageJ program (table). The experiment is representative of three performed with similar results.

synapse, SNX27 itself could be important to attract DGKζ to the immunological synapse and/or to endosomal compartments where it will regulate DAG levels and, ultimately, TCR signals. Indeed, SNX27 silencing mirrors the activation of the ERK pathway that is observed in DGKζ knockdown cells, strongly suggesting that both proteins act in the same pathway. These results are better understood when examined in relation to the mechanisms by which DAG membrane levels modulate Ras activation in T cells. Studies in Jurkat T cells have elegantly shown that DAG-dependent activation of RasGRP1 is important to induce a positive-feedback loop, priming SOS activation (Roose et al., 2007). The interplay between these two RasGEF proteins has been the basis for theoretical models that explain how lymphocytes can adopt specific responses to antigens with different affinities to the TCR (Das et al., 2009).

The regulation of RasGRP1 by a membrane lipid not only provides a sophisticated mechanism that translates affinity of the receptor into signal strength, but could also provide a mechanism for Ras signalling compartmentalisation, a matter that has recently received considerable attention (Mor and Philips, 2006). Whereas SOS activates Ras exclusively at the plasma membrane, RasGRP1 can also function in internal membranes providing a mechanism to activate Ras localised to endosomes (Daniels et al., 2006). DGKζ limits the threshold of T cell activation by metabolising the DAG required to activate RasGRP1 (Roose et al., 2005), but there is no information available regarding the spatial regulation of DGKζ following TCR triggering. Our data not only shows a common role for SNX27 and DGKζ as negative modulators of ERK phosphorylation, but also suggests a role for SNX27 in the complex and still unresolved mechanism by which DGKζ regulates the Ras–ERK pathway.

Our data showing PDZ-independent recruitment of DGKζ to the entire plasma membrane as a consequence of T cell-APC interaction, are reminiscent of the dynamic translocation of this enzyme in response to ectopically expressed muscarinic type I receptors (Santos et al., 2002). Recent studies showed that DAG and proteins bearing DAG-binding motifs have a key role in different steps of immunological synapse formation, including MTOC reorientation, immunological synapse breakdown and granule polarisation (Ma et al., 2008; Quann et al., 2009; Sims et al., 2007). DGKζ dissociation from the endocytic/recycling compartment as a consequence of APC contact would facilitate membrane DAG elevation in this membrane compartment.

Overall, the data presented in this paper support a model in which feedback between SNX27 and DGKζ ensures the spatial recruitment of both proteins to sites of active signalling. The identification of SNX27 as a DGKζ partner and the characterisation of its relocation during immunological synapse formation allow us to postulate a previously unreported function in T cell activation for this member of the sorting nexin family. These data shed new light on the dynamic regulation of SNX27 and DGKζ in T cells and provide additional evidence on the important role of membrane trafficking in the regulation of T cell functions.

Materials and Methods
Antibodies
Anti-DGKζ (N-terminal peptide) was a generous gift from Matthew Topham (University of Utah, Salt Lake City, UT) (Abramovici et al., 2003), anti-SNX27 was previously described (Rincon et al., 2007) anti-phosphorylated MAPK (pERK1+pERK2, Cell Signaling), anti-haemagglutinin (anti-HA; Babco), anti-GST (Santa Cruz Biotechnology), anti-SNX2 and anti-PKCθ (BD Transduction Laboratories), anti-human-CD3 and -CD28 (BD Pharmingen), anti-tubulin (Sigma) and anti-phosphotyrosine (Upstate Biotechnology), anti-human-TfR and -MAPK (ERK1+ERK2) (Zymed Laboratories). Monoclonal antibodies against human Lamp1 (developed by Thomas August and James E. K. Hildreth) was obtained from the Developmental Studies Hybridoma Bank (developed under the auspices of the NICHD and maintained by the Univ. Iowa Dept Biological Sciences, Iowa City, IA). Mouse anti-LFA-1 and -CD3 (clone T3b for lipid planar bilayer assays and clone OKT3 for IF analysis) were a generous gift from Miguel A. Alonso (CBMSO, Madrid, Spain) and Francisco Sánchez-Madrid (Hospital de la Princesa, Madrid, Spain), respectively.

Plasmids and DNA constructs
HA–DGKζCT, GFP–RasGRP1 and human Myc-tagged SNX27ΔRA, mouse green fluorescence protein (GFP)-tagged SNX27 and SNX27ΔPDZ were previously described (Carrasco and Merida, 2004; Rincon et al., 2007; Santos et al., 2002). GFP–PKCθ was from Clontech. To generate GFP–SNX27(R$_{196}$A,Y$_{197}$A), the (559)CGGTAC(564) sequence in GFP–SNX27 was mutated to GCGGCC. To generate RFP–DGKζ, pcDNA3MycDGKζ (Santos et al., 2002) was digested with KpnI and BglII and the 2.9 kb fragment was subcloned into the KpnI–BglII site of the mRFP expression vector (kindly provided by Santos Mañes, Centro Nacional de Biotecnología, Madrid, Spain). To generate the PDZ-binding motif deletion mutant (RFP–DGKζΔPDZbm), the (2776)GAG(2778) sequence in RFP–DGKζ was mutated to TAG. Site-directed mutagenesis was performed using the QuikChange mutagenesis kit (Stratagene). To generate GST fusion proteins, GFP–SNX27, GFP–SNX27(R$_{196}$A,Y$_{197}$A) and GFP–SNX27ΔPDZ were digested with SalI and NotI and the 1.7 kb (1.35 kb for SNX27ΔPDZ) fragments were subcloned in the pGEX4T1 vector digested with SalI and NotI, generating GST–SNX27, GST–SNX27(R$_{196}$A,Y$_{197}$A) and GST–SNX27ΔPDZ. All constructs were confirmed by sequencing.

siRNA knockdown of DGKζ and SNX27
Silencing of DGKζ was performed as reported (Rincon et al., 2007). The mouse DGKα sequence (nucleotides 1153–1173) was used as control (pSUPER-RNAi-

Control). For ERK phosphorylation analysis, we purchased the silencer negative control 1 siRNA and a pre-designed siRNA against human SNX27 (siRNA ID: 131018) from Ambion; for DGKζ knockdown in this analysis, we selected the 21-nucleotide sequence mentioned above.

Cell lines and transient transfection

Jurkat T cells (human acute T cell leukaemia) in logarithmic growth phase were transfected (1.2×10^7 in 400 μl complete medium) with 20 μg plasmid DNA by electroporation with a Gene Pulser (Bio-Rad; 270 V, 975 μF); cells were assayed 24 hours after transfection. For RNAi of DGKζ and SNX27, 1.2×10^7 Jurkat T cells were transfected in 400 μl of OptiMEM (Gibco, Invitrogen Life Technologies) with 5 μg siRNA by electroporation at 250 V, 950 μF) and cells were assayed at 72 hours after transfection. Raji B cells (human B cell lymphoma), used as APCs, were maintained in RPMI 1640 medium (BioWhittaker) with 10% FBS and 2 mM glutamine.

Stimulation with anti-CD3 and anti-CD28 fibronectin-coated plates or CD3 and CD28 beads

Slides were precoated with a 1:1 mixture of anti-CD3 and anti-CD28 (10 μg/ml each) in PBS or with fibronectin (10 μg/ml) in PBS for 1 hour at 37°C and washed three times with PBS. Transfected Jurkat cells were plated onto slides (20 minutes) then examined by confocal microscopy. To stimulate with antibody-coated beads, polystyrene microspheres (15.0 μm, from Polysciences) were pre-coated with anti-CD3 and anti-CD28, as previously described (Carrasco and Merida, 2004). For stimulation, 0.4×10^5 transfected Jurkat cells were mixed with antibody-coated beads at a 1:1 cell:bead ratio and plated on chambered coverslips. After 20 minutes, images were captured by confocal microscopy.

Stimulation with antigen-presenting cells

Raji B cells were stained with 50 μM CMAC and were pulsed with medium alone or with 1 μg/ml bacterial superantigen *Staphylococcus* enterotoxin E (SEE) (Toxin Technology) (Fraser et al., 2000) (1 hour, 37°C); Raji cells were washed in complete medium and then mixed 1:1 with Jurkat T cells. For primaquine treatment, Jurkat T cells were incubated with medium alone or with 300 μM primaquine (15 minute, 37°C) before mixing with Raji cells. Cell–cell conjugates were imaged by confocal microscopy or processed for immunofluorescence analysis. For MAPK activation analysis, Jurkat T cells transiently transfected with selected siRNA, were stimulated with Raji B cells (1:1) unpulsed (time 0) or pulsed (times 5 and 15 minutes). After treatment, cells were pelleted and lysed for western blot analysis.

Western blot

Jurkat cells, transiently transfected with selected plasmids or siRNA, were lysed in NP40 buffer (150 mM NaCl, 10 mM NaF, 10 mM Na$_4$P$_2$O$_7$, 50 mM Tris-HCl, pH 7.5, 1% Igepal CA-630 and 0.5 mM PMSF/protease inhibitor cocktail); lysates were incubated (15 minutes, on ice) and centrifuged (20,800 **g**, 10 minutes, 4°C). Following protein assay (DC protein assay, Bio-Rad), equivalent protein amount per sample was analysed by SDS-PAGE. Proteins were transferred to nitrocellulose membrane, incubated with specified antibodies, and detected using the ECL detection kit (Amersham Bioscience).

Lipid-binding assay

GST-tagged SNX27 constructs were produced in *Escherichia coli* strain BL21(De3)pLysS by standard procedures. GST alone was used as control. Protein-rich fractions were collected and concentrated using Amicon Ultra-4 centrifugal filter devices (Millipore). Protein concentration was determined and the GST-recombinant proteins were used for lipid-binding studies. PIP Strips (Molecular Probes) were probed with 0.5 μg/ml GST-tagged fusion protein following the manufacturer's instructions.

Immunofluorescence analysis

Cells were transferred to poly-DL-lysine-coated coverslips and allowed to attach (30 minutes). Where indicated, attached cells were serum-starved (30 minutes) and incubated with transferrin–Rhodamine (Tf-Rhod) (20 μg/ml, 15–30 minutes, 37°C). Cells were fixed for 4 minutes in cold methanol (10 minutes in 2% paraformaldehyde to visualise RFP–DGKζFL or RFP–GDKζΔPDZbm), then washed with phosphate-buffered saline (PBS) and blocked in PBS, 3% FBS for 15 minutes at room temperature. Primary antibodies (diluted 1:100 in PBS with 3% FBS) were incubated (1 hour, 37°C) and washed with PBS; the same procedure was followed for secondary antibodies. Cells mounted on glass slides were imaged with an Olympus Fluoview FV-1000 laser-scanning confocal microscope. Images were processed using ImageJ (National Institutes of Health; http://rsb.info.nih.gov/ij/index.html) and Adobe Photoshop software. For quantitative analysis of SNX27 and DGKζ distribution at the plasma membrane, fluorescence signals were profiled along a line at the equatorial plane of the cell using the ImageJ program. The colocalisation plots and the Pearson´s correlation coefficients (Bolte and Cordelieres, 2006) were also produced with ImageJ. Three-dimensional (3D) reconstructions of confocal sections (0.250 μm separation in the vertical axis, acquired on a Zeiss Axiovert LSM 510-META inverted microscope) were assembled with Imaris 6.0 software (Bitplane).

Time-lapse microscopy imaging

At 24 hours after transfection, cells were transferred to chambered coverslips coated with poly-DL-lysine, fibronectin or anti-CD3 and anti-CD28 (Nunc LabTek), allowed to attach for at least 20 minutes at 37°C, washed and maintained in HEPES-buffered Hanks' balanced salt solution (HBSS; 25 mM HEPES-KOH, pH 7.4, 1 mM MgCl$_2$, 1 mM CaCl$_2$, 132 mM NaCl, 0.1% BSA) supplemented with 2% FBS. Cells were placed on a heated plate and were time-lapse imaged every 20 seconds with an Olympus confocal microscope; pulsed and stained APCs were added during acquisition. Images were processed using ImageJ and Adobe Photoshop.

Analysis of protein accumulation at the T-cell–APC contact area

To quantify the amount of GFP–SNX27 accumulated at the immunological synapse compared with the total GFP–SNX27, Z-series optical sections (0.2 μm) were recorded. Four or five contiguous optical sections were stacked and contained all the three-dimensional fluorescence information. To analyse these stacks, we devised a plug-in for ImageJ that allows us to measure the average fluorescent intensity in the background (Bg), at the whole cell (Cell) and in the region of interest (ROI). Then, we compute the intensity ratio as $Z=(ROI-Bg)/(Cell-Bg)$. To quantify protein accumulation at the immunological synapse compared with other regions of plasma membrane of the T cell, we designed another plugin for ImageJ, which measures the average intensity value of the image in small circles at the background (Bg), the plasma membrane of the T cell outside the immunological synapse (T) and the synapse (S) when the fluorescent protein is expressed by only one of the two cells. For each measurement (Bg, T and S) the average pixel value was computed. From these observed values, we separate the contribution of each one of the components (background, constitutive T cell and T cell at the synapse). Finally, we computed the ratio between the fluorescence at the synapse and outside the synapse. Ratio values were represented as dot plots, with each dot representing the value of an individual cell.

Planar lipid bilayers

The planar lipid bilayers were formed on FCS2 flow chambers as previously described (Grakoui et al., 1999). Briefly, unlabeled GPI-linked ICAM-1 (inter-cellular adhesion molecule 1) liposomes and biotinylated lipids were mixed with 1,2-dioleoyl-PC (DOPC) lipids (Avanti Polar Lipids) at different ratios to get the molecular density required. Once the planar bilayers formed, the chambers were blocked with PBS 2% FBS for 1 hour at room temperature, followed by antigen loading in PBS 0.5% FBS. Monobiotinylated anti-human CD3 antibody (clone T3b) was tethered on the lipid bilayers as surrogate antigen, previous incubation with Alexa Fluor 647 streptavidin (Molecular Probes). T cells were injected into the warmed (37°C) chamber at time zero, and then followed over the time by confocal fluorescence microscopy. The assays were done in PBS with 0.5% FBS, 2 mM Mg^{2+}, 0.5 mM Ca^{2+}, 1 g/l D-glucose at 37°C. Images were acquired on a Zeiss Axiovert LSM 510-META inverted microscope with a 40× oil-immersion objective and analysed by LSM 510 software (Zeiss, Germany) and Imaris 6.0 software (Bitplane). To quantify the frequency of cells that exhibit protein accumulation at the immunological synapse, we acquired images 25 minutes after cell injection.

Statistical analysis

To analyse the fluorescence intensity data of SNX27 at the immunological synapse, we used a two-sample Kolmogorov-Smirnov test to compare pairs of distributions of ratios from different cells. We applied a Bonferroni correction to the confidence thresholds to account for the multiple comparisons performed. Differences between two cell frequency means were tested by Student's *t*-tests using PRISM software. Differences were considered not significant (ns) when $P>0.05$, significant (*) when $P<0.05$, very significant (**) when $P<0.01$ and extremely significant (***) when $P<0.001$.

References

Abramovici, H., Hogan, A., Obagi, C., Topham, M. and Gee, S. (2003). Diacylglycerol kinase-zeta localization in skeletal muscle is regulated by phosphorylation and interaction with syntrophins. *Mol. Biol. Cell* **14**, 4499-4511.

Anton, O., Batista, A., Millan, J., Andres-Delgado, L., Puertollano, R., Correas, I. and Alonso, M. A. (2008). An essential role for the MAL protein in targeting Lck to the plasma membrane of human T lymphocytes. *J. Exp. Med.* **205**, 3201-3213.

Badour, K., McGavin, M. K., Zhang, J., Freeman, S., Vieira, C., Filipp, D., Julius, M., Mills, G. B. and Siminovitch, K. A. (2007). Interaction of the Wiskott-Aldrich syndrome protein with sorting nexin 9 is required for CD28 endocytosis and cosignaling in T cells. *Proc. Natl. Acad. Sci. USA* **104**, 1593-1598.

Billadeau, D. D., Nolz, J. C. and Gomez, T. S. (2007). Regulation of T cell activation by the cytoskeleton. *Nat. Rev. Immunol.* **7**, 131-143.

Blott, E. J. and Griffiths, G. M. (2002). Secretory lysosomes. *Nat. Rev. Mol. Cell Biol.* **3**, 122-131.

Bolte, S. and Cordelieres, F. P. (2006). A guided tour into subcellular colocalization analysis in light microscopy. *J. Microsc.* **224**, 213-232.

Bonello, G., Blanchard, N., Montoya, M. C., Aguado, E., Langlet, C., He, H. T., Nunez-Cruz, S., Malissen, M., Sanchez-Madrid, F., Olive, D. et al. (2004). Dynamic recruitment of the adaptor protein LAT: LAT exists in two distinct intracellular pools and controls its own recruitment. *J. Cell Sci.* **117**, 1009-1016.

Bravo, J., Karathanassis, D., Pacold, C., Pacold, M., Ellson, C., Anderson, K. E., Butler, P., Lavenir, I., Perisic, O., Hawkins, P. T. et al. (2001). The crystal structure of the PX domain from p40(phox) bound to phosphatidylinositol 3-phosphate. *Mol. Cell* **8**, 829-839.

Carlton, J., Bujny, M., Rutherford, A. and Cullen, P. (2005). Sorting nexins- unifying trends and perspectives. *Traffic* **6**, 75-82.

Carrasco, S. and Merida, I. (2004). Diacylglycerol-dependent binding recruits PKCtheta and RasGRP1 C1 domains to specific subcellular localizations in living T lymphocytes. *Mol. Biol. Cell* **15**, 2932-2942.

Cemerski, S. and Shaw, A. (2006). Immune synapses in T-cell activation. *Curr. Opin. Immunol.* **18**, 298-304.

Chen, J. W., Cha, Y., Yuksel, K. U., Gracy, R. W. and August, J. T. (1988). Isolation and sequencing of a cDNA clone encoding lysosomal membrane glycoprotein mouse LAMP-1. Sequence similarity to proteins bearing onco-differentiation antigens. *J. Biol. Chem.* **263**, 8754-8758.

Cullen, P. J. (2008). Endosomal sorting and signalling: an emerging role for sorting nexins. *Nat. Rev. Mol. Cell Biol.* **9**, 574-582.

Daniels, M. A., Teixeiro, E., Gill, J., Hausmann, B., Roubaty, D., Holmberg, K., Werlen, G., Hollander, G. A., Gascoigne, N. R. and Palmer, E. (2006). Thymic selection threshold defined by compartmentalization of Ras/MAPK signalling. *Nature* **444**, 724-729.

Das, J., Ho, M., Zikherman, J., Govern, C., Yang, M., Weiss, A., Chakraborty, A. K. and Roose, J. P. (2009). Digital signaling and hysteresis characterize ras activation in lymphoid cells. *Cell* **136**, 337-351.

Das, V., Nal, B., Dujeancourt, A., Thoulouze, M. I., Galli, T., Roux, P., Dautry-Varsat, A. and Alcover, A. (2004). Activation-induced polarized recycling targets T cell antigen receptors to the immunological synapse; involvement of SNARE complexes. *Immunity* **20**, 577-588.

Davis, M. M., Krogsgaard, M., Huppa, J. B., Sumen, C., Purbhoo, M. A., Irvine, D. J., Wu, L. C. and Ehrlich, L. (2003). Dynamics of cell surface molecules during T cell recognition. *Annu. Rev. Biochem.* **72**, 717-742.

Dustin, M. L., Starr, T., Varma, R. and Thomas, V. K. (2007). Supported planar bilayers for study of the immunological synapse. *Curr. Protoc. Immunol.* **Chapter 18**, Unit 18.13.

Ehrlich, L. I., Ebert, P. J., Krummel, M. F., Weiss, A. and Davis, M. M. (2002). Dynamics of p56lck translocation to the T cell immunological synapse following agonist and antagonist stimulation. *Immunity* **17**, 809-822.

Fabre, S., Reynaud, C. and Jalinot, P. (2000). Identification of functional PDZ domain binding sites in several human proteins. *Mol. Biol. Rep.* **27**, 217-224.

Fooksman, D. R., Vardhana, S., Vasiliver-Shamis, G., Liese, J., Blair, D. A., Waite, J., Sacristan, C., Victora, G. D., Zanin-Zhorov, A. and Dustin, M. L. (2010). Functional anatomy of T cell activation and synapse formation. *Annu. Rev. Immunol.* **28**, 79-105.

Fraser, J., Arcus, V., Kong, P., Baker, E. and Proft, T. (2000). Superantigens-powerful modifiers of the immune system. *Mol. Med. Today* **6**, 125-132.

Friedl, P. and Gunzer, M. (2001). Interaction of T cells with APCs: the serial encounter model. *Trends Immunol.* **22**, 187-191.

Friedl, P. and Storim, J. (2004). Diversity in immune-cell interactions: states and functions of the immunological synapse. *Trends Cell Biol.* **14**, 557-567.

Friedl, P., den Boer, A. T. and Gunzer, M. (2005). Tuning immune responses: diversity and adaptation of the immunological synapse. *Nat. Rev. Immunol.* **5**, 532-545.

Giallourakis, C., Cao, Z., Green, T., Wachtel, H., Xie, X., Lopez-Illasaca, M., Daly, M., Rioux, J. and Xavier, R. (2006). A molecular-properties-based approach to understanding PDZ domain proteins and PDZ ligands. *Genome Res.* **16**, 1056-1072.

Gillooly, D. J., Morrow, I. C., Lindsay, M., Gould, R., Bryant, N. J., Gaullier, J. M., Parton, R. G. and Stenmark, H. (2000). Localization of phosphatidylinositol 3-phosphate in yeast and mammalian cells. *EMBO J.* **19**, 4577-4588.

Grakoui, A., Bromley, S. K., Sumen, C., Davis, M. M., Shaw, A. S., Allen, P. M. and Dustin, M. L. (1999). The immunological synapse: a molecular machine controlling T cell activation. *Science* **285**, 221-227.

Gullapalli, A., Garrett, T. A., Paing, M. M., Griffin, C. T., Yang, Y. and Trejo, J. (2004). A role for sorting nexin 2 in epidermal growth factor receptor down-regulation: evidence for distinct functions of sorting nexin 1 and 2 in protein trafficking. *Mol. Biol. Cell* **15**, 2143-2155.

Hiebsch, R. R., Raub, T. J. and Wattenberg, B. W. (1991). Primaquine blocks transport by inhibiting the formation of functional transport vesicles. Studies in a cell-free assay of protein transport through the Golgi apparatus. *J. Biol. Chem.* **266**, 20323-20328.

Hogan, A., Shepherd, L., Chabot, J., Quenneville, S., Prescott, S. M., Topham, M. K. and Gee, S. H. (2001). Interaction of gamma 1-syntrophin with diacylglycerol kinase-zeta. Regulation of nuclear localization by PDZ interactions. *J. Biol. Chem.* **276**, 26526-26533.

Huse, M., Lillemeier, B. F., Kuhns, M. S., Chen, D. S. and Davis, M. M. (2006). T cells use two directionally distinct pathways for cytokine secretion. *Nat. Immunol.* **7**, 247-255.

Huse, M., Quann, E. J. and Davis, M. M. (2008). Shouts, whispers and the kiss of death: directional secretion in T cells. *Nat. Immunol.* **9**, 1105-1111.

Joubert, L., Hanson, B., Barthet, G., Sebben, M., Claeysen, S., Hong, W., Marin, P., Dumuis, A. and Bockaert, J. (2004). New sorting nexin (SNX27) and NHERF specifically interact with the 5-HT4a receptor splice variant: roles in receptor targeting. *J. Cell Sci.* **117**, 5367-5379.

Kim, E. and Sheng, M. (2004). PDZ domain proteins of synapses. *Nat. Rev. Neurosci.* **5**, 771-781.

Kim, K., Yang, J., Zhong, X. P., Kim, M. H., Kim, Y. S., Lee, H. W., Han, S., Choi, J., Han, K., Seo, J. et al. (2009). Synaptic removal of diacylglycerol by DGKzeta and PSD-95 regulates dendritic spine maintenance. *EMBO J.* **28**, 1170-1179.

Lee, K. H., Dinner, A. R., Tu, C., Campi, G., Raychaudhuri, S., Varma, R., Sims, T. N., Burack, W. R., Wu, H., Wang, J. et al. (2003). The immunological synapse balances T cell receptor signaling and degradation. *Science* **302**, 1218-1222.

Ludford-Menting, M. J., Oliaro, J., Sacirbegovic, F., Cheah, E. T., Pedersen, N., Thomas, S. J., Pasam, A., Iazzolino, R., Dow, L. E., Waterhouse, N. J. et al. (2005). A network of PDZ-containing proteins regulates T cell polarity and morphology during migration and immunological synapse formation. *Immunity* **22**, 737-748.

Lunn, M. L., Nassirpour, R., Arrabit, C., Tan, J., McLeod, I., Arias, C. M., Sawchenko, P. E., Yates, J. R., III and Slesinger, P. A. (2007). A unique sorting nexin regulates trafficking of potassium channels via a PDZ domain interaction. *Nat. Neurosci.* **10**, 1249-1259.

Ma, J. S., Haydar, T. F. and Radoja, S. (2008). Protein kinase C delta localizes to secretory lysosomes in CD8+ CTL and directly mediates TCR signals leading to granule exocytosis-mediated cytotoxicity. *J. Immunol.* **181**, 4716-4722.

MacNeil, A. J. and Pohajdak, B. (2007). Polarization of endosomal SNX27 in migrating and tumor-engaged natural killer cells. *Biochem. Biophys. Res. Commun.* **361**, 146-150.

MacNeil, A. J., Mansour, M. and Pohajdak, B. (2007). Sorting nexin 27 interacts with the Cytohesin associated scaffolding protein (CASP) in lymphocytes. *Biochem. Biophys. Res. Commun.* **359**, 848-853.

Maxfield, F. R. and McGraw, T. E. (2004). Endocytic recycling. *Nat. Rev. Mol. Cell Biol.* **5**, 121-132.

Monks, C. R., Kupfer, H., Tamir, I., Barlow, A. and Kupfer, A. (1997). Selective modulation of protein kinase C-theta during T-cell activation. *Nature* **385**, 83-86.

Monks, C. R., Freiberg, B. A., Kupfer, H., Sciaky, N. and Kupfer, A. (1998). Three-dimensional segregation of supramolecular activation clusters in T cells. *Nature* **395**, 82-86.

Mor, A. and Philips, M. R. (2006). Compartmentalized Ras/MAPK signaling. *Annu. Rev. Immunol.* **24**, 771-800.

Olenchock, B. A., Guo, R., Carpenter, J. H., Jordan, M., Topham, M. K., Koretzky, G. A. and Zhong, X. P. (2006). Disruption of diacylglycerol metabolism impairs the induction of T cell anergy. *Nat. Immunol.* **7**, 1174-1181.

Quann, E. J., Merino, E., Furuta, T. and Huse, M. (2009). Localized diacylglycerol drives the polarization of the microtubule-organizing center in T cells. *Nat. Immunol.* **10**, 627-635.

Rincon, E., Santos, T., Avila-Flores, A., Albar, J. P., Lalioti, V., Lei, C., Hong, W. and Merida, I. (2007). Proteomics identification of sorting nexin 27 as a diacylglycerol kinase zeta-associated protein: new diacylglycerol kinase roles in endocytic recycling. *Mol. Cell. Proteomics* **6**, 1073-1087.

Roose, J. P., Mollenauer, M., Gupta, V. A., Stone, J. and Weiss, A. (2005). A diacylglycerol-protein kinase C-RasGRP1 pathway directs Ras activation upon antigen receptor stimulation of T cells. *Mol. Cell. Biol.* **25**, 4426-4441.

Roose, J. P., Mollenauer, M., Ho, M., Kurosaki, T. and Weiss, A. (2007). Unusual interplay of two types of Ras activators, RasGRP and SOS, establishes sensitive and robust Ras activation in lymphocytes. *Mol. Cell. Biol.* **27**, 2732-2745.

Sanjuan, M. A., Pradet-Balade, B., Jones, D. R., Martinez, A. C., Stone, J. C., Garcia-Sanz, J. A. and Merida, I. (2003). T cell activation in vivo targets diacylglycerol kinase alpha to the membrane: a novel mechanism for Ras attenuation. *J. Immunol.* **170**, 2877-2883.

Santos, T., Carrasco, S, Jones, D. R., Merida, I. and Eguinoa, A. (2002). Dynamics of DGKzeta translocation in living T cells. Study of the structural domain requirements for translocation and activity. *J. Biol. Chem.* **277**, 30300-30309.

Sheng, M. and Sala, C. (2001). PDZ domains and the organization of supramolecular complexes. *Annu. Rev. Neurosci.* **24**, 1-29.

Sims, T. N., Soos, T. J., Xenias, H. S., Dubin-Thaler, B., Hofman, J. M., Waite, J. C., Cameron, T. O., Thomas, V. K., Varma, R., Wiggins, C. H. et al. (2007). Opposing effects of PKCtheta and WASp on symmetry breaking and relocation of the immunological synapse. *Cell* **129**, 773-785.

Somasundaram, B., Norman, J. C. and Mahaut-Smith, M. P. (1995). Primaquine, an inhibitor of vesicular transport, blocks the calcium-release-activated current in rat megakaryocytes. *Biochem. J.* **309**, 725-729.

Stahelin, R. V., Digman, M. A., Medkova, M., Ananthanarayanan, B., Rafter, J. D., Melowic, H. R. and Cho, W. (2004). Mechanism of diacylglycerol-induced

membrane targeting and activation of protein kinase Cdelta. *J. Biol. Chem.* **279**, 29501-29512.

van der Merwe, P. A. (2002). Formation and function of the immunological synapse. *Curr. Opin. Immunol.* **14**, 293-298.

van Weert, A. W., Geuze, H. J., Groothuis, B. and Stoorvogel, W. (2000). Primaquine interferes with membrane recycling from endosomes to the plasma membrane through a direct interaction with endosomes which does not involve neutralisation of endosomal pH nor osmotic swelling of endosomes. *Eur. J. Cell Biol.* **79**, 394-399.

Wang, H., Lim, D. and Rudd, C. E. (2010). Immunopathologies linked to integrin signalling. *Semin. Immunopathol.* **32**, 173-182.

Worby, C. A. and Dixon, J. E. (2002). Sorting out the cellular functions of sorting nexins. *Nat. Rev Mol. Cell Biol.* **3**, 919-931.

Xu, Y., Hortsman, H., Seet, L., Wong, S. H. and Hong, W. (2001). SNX3 regulates endosomal function trough its PX-domain-mediated interaction with PtdIns(3)P. *Nat. Cell Biol.* **3**, 658-667.

Yokosuka, T., Kobayashi, W., Sakata-Sogawa, K., Takamatsu, M., Hashimoto-Tane, A., Dustin, M. L., Tokunaga, M. and Saito, T. (2008). Spatiotemporal regulation of T cell costimulation by TCR-CD28 microclusters and protein kinase C theta translocation. *Immunity* **29**, 589-601.

Zhong, X., Hainey, E. A., Olenchock, B. A., Jordan, M. S., Maltzman, J. S., Nichols, K. E., Shen, H. and Koretzky, G. A. (2003). Enhanced T cell responses due to diacylglycerol kinase zeta deficiency. *Nat. Immunol.* **4**, 882-890.

Zhong, X. P., Hainey, E. A., Olenchock, B. A., Zhao, H., Topham, M. K. and Koretzky, G. A. (2002). Regulation of T cell receptor-induced activation of the Ras-ERK pathway by diacylglycerol kinase zeta. *J. Biol. Chem.* **277**, 31089-31098.